THE EFFECTS OF REFLECTING SURFACE MATERIAL PROPERTIES ON TIME-OF-FLIGHT LASER SCANNER MEASUREMENTS

D D Lichti
Department of Spatial Sciences
Curtin University of Technology
GPO Box U1987
Perth, WA 6845
AUSTRALIA

B R Harvey
School of Surveying and Spatial Information Systems
The University of New South Wales
Sydney, NSW 2052
AUSTRALIA

Abstract

Terrestrial laser scanners, such as the Cyrax 2500 and its predecessor the 2400, use pulsed laser ranging and rotating mirrors to accurately measure dense sets of three-dimensional co-ordinates of entire surfaces. Range is observed by measuring the two-way time of flight (TOF) of the reflected laser pulse. The reflectorless nature of the rangefinder raises the possibility of range errors due to pulse attenuation by the reflecting surface. This paper reports on an investigation into the effects of reflecting surface properties on TOF laser scanner measurements made with a Cyrax 2400. Tests were conducted at close range (3m) and medium range (53m). Several samples of construction materials and rocks from Western Australia having various surface roughness and mineral composition were tested with both dry and wet reflecting surfaces. Results presented show no significant range errors due to differing material properties, but do exhibit changes in range measurement distribution and return signal intensity.

Key words: laser scanning, surface reflectance, time-of-flight ranging.

1. Introduction

Ground-based laser scanning is an emerging technology that is attracting a great deal of interest within several areas of geomatics. The high temporal scanning frequency, high spatial point density, accuracy and reflectorless nature of scanning systems are some of the salient properties attracting the attention. Documented applications include deformation monitoring (Lichti *et al.*, 2000), structural assessment of a bridge (Gordon *et al.*, 2001), landslide monitoring (Kurisake *et al.*, 2001), ice cave mapping (Ullrich *et al.*, 2001), mapping the interior of buildings (Runne *et al.*, 2001) and building façade measurement (Balzani *et al.*, 2001; Ullrich *et al.*, 2001).

A time-of-flight (TOF) system measures range, ρ, by observing the two-way travel time, Δt, of a short (5-50ns in duration; Amann *et al.*, 2001) pulse of laser light,

$$\rho = \frac{1}{2} c \Delta t \tag{1}$$

where c is the velocity of light. The reflectorless nature of the rangefinder means there is no need to place retro-reflective targets on the object to be measured. Range to the surface is measured provided that a sufficient amount of pulse energy is reflected so as to register a signal with the scanner's photodetector. The current generated by the detector must exceed a predefined threshold in order for the return time to be observed.

In considering reflectorless TOF measurement systems, a question that naturally arises is: What is the influence of the reflecting surface material properties? Two aspects of this question must be considered. The first is the effect on the maximum range that can be measured. Neglecting atmospheric effects, reflection-related energy losses may be attributed to diffuse scattering, absorption and transmission if the material is translucent. Ullrich *et al.* (2001) provide a plot of maximum range as a function of reflectivity for the RIEGL scanner (λ=900nm). As might be expected, the curve shows that maximum range to materials with low reflectivity (e.g., coal) is considerably low in relation to highly reflective materials such as white masonry.

The second aspect is the range delay error, $\delta\rho$, corresponding to a timing error, δt, caused by the attenuated amplitude of the reflected laser pulse. Godin *et al.* (2001) demonstrate a small (40μm) range bias due to subsurface scattering in translucent marble for an active laser triangulation system (i.e., not a TOF system). Gordon *et al.* (2001) report on errors in

Cyrax 2400 range measurements from retro-reflective targets thought to be due to photodetector saturation. It is acknowledged that any effect from non-retro targets is unlikely to be of consequence for applications such as as-built surveys and stockpile volume measurement. However, as laser-scanning technology becomes more widely available and accepted, it is increasingly likely to be applied to projects demanding greater accuracy for which such range errors may be of significance.

This paper reports the findings of an investigation into the effects of reflecting surface properties on TOF laser scanner measurements. Numerous rock and construction material samples with different surface roughness, mineral composition and colour were tested. Tests were performed on each specimen with both dry and wet reflecting surfaces. A variety of surveying reflectors was also scanned. Testing was conducted at close and medium range. Following a review of reflection of electromagnetic radiation (EMR), the experiment details are described. Quantitative assessment of the effects on reflecting surface on both range and return signal intensity are then presented, followed by conclusions.

2. Reflection of Electromagnetic Radiation

The reflectance of a particular sample is governed by incidence angle, surface roughness and the material properties, which include electric permittivity, magnetic permeability and conductivity (Jelalian, 1992). Various measures exist to quantify reflectance, such as specular, hemispherical and bi-directional (Wolfe, 1998). Here, measures based upon material properties of the reflecting surface are reviewed.

Considering the case of specular reflection from a smooth surface at normal incidence, the coefficient of reflection, r, is given by (Fowles, 1975)

$$r = \frac{E_r}{E_i} = \frac{1 - N}{1 + N} \tag{2}$$

and the reflectance, R, is given by

$$R = \frac{(1 - N)(1 - N)^*}{(1 + N)(1 + N)^*} \tag{3}$$

where

E_i is the amplitude of the incident electric field;

E_r is the amplitude of the reflected electric field;

$*$ indicates complex conjugation; and

N is the complex index of refraction, given by

$$N = n + j\kappa \tag{4}$$

where

n is the refractive index of the material;

κ is the extinction index; and

$$j = \sqrt{-1}\ .$$

Since the current produced by an optical detector in response to an incident electromagnetic field is proportional to the square of the amplitude (i.e., the power; Wolfe, 1998), Eq. 3 is the most relevant measure of reflectance for the present discussion.

The refractive index, defined as the ratio of the velocity of light in a vacuum to that in a given medium, is a function of the electric permittivity and magnetic permeability (Fowles, 1975),

$$n = \sqrt{KK_m} \tag{5}$$

where

K is the relative electric permittivity; and

K_m is the relative magnetic permeability.

The extinction index determines how much EMR is absorbed by the medium, and is given by (Fowles, 1975)

$$\kappa = \alpha \frac{c}{\omega} \tag{6}$$

where

α is the coefficient of absorption; and

ω is the frequency of the EMR.

For a dielectric (insulator) material, the extinction index approaches zero so the refractive index is real and the reflectance becomes

$$R = \frac{(1-n)^2}{(1+n)^2} \tag{7}$$

For conducting media (e.g., metals), the extinction index is large and both it and the refractive index also depend upon electric conductivity, σ. For a non-magnetic medium, the relative permeability is unity, so the refractive index is solely a function of the electric permittivity. The specimens tested in this study fall under the category of non-magnetic dielectrics.

3. Experiment Description

To quantify the effects--if any--of reflecting surface material properties on pulsed laser range measurements, an experiment was conducted using the University of New South Wales School of Surveying and Spatial Information Systems' Cyrax 2400 (predecessor to the 2500) laser scanner. The Cyrax 2400 offers ±4mm range-accuracy, ±60μrad (12") angular accuracy and maximum range of about 100m. Co-ordinate accuracy is quoted as ±6mm up to a range of 50m. Rotating mirrors deflect the green laser (λ=532nm) pulse to provide measurement of three-dimensional co-ordinates referenced to the scanner's internal co-ordinate system. In addition to the co-ordinates, the Cyrax also provides a unitless, normalised measure of return signal energy—loosely termed intensity—that ranges between 0 and 1.

Several different hand-sized rock specimens and construction materials (brick, concrete and limestone block) collected from around Western Australia were scanned. Table 1 provides a summary of each specimen, including colour, composition, approximate planar surface area scanned and a qualitative description of the planar surface roughness. The chosen samples provided a variety of colours and mineral compositions for the study. Some were taken from North Dandalup dam southeast of Perth, the subject of a previous scanning campaign with a near infrared scanner (Lichti *et al.*, 2000). Others were taken from the Curtin University campus, where in another study (Gordon *et al.*, 2001), a scanner similar to the one described above was unable to register returns from the construction materials, in particular the red brick. Thus, there was much interest in their measurement in this study.

Table 1. Summary of Specimens.

Specimen	Colour of Planar Surface and Composition	Planar Surface Area (cm^2)	Planar Surface Finish
Red Brick	Homogeneous: brownish red; opaque	86	Smooth
Limestone	Homogeneous: white; opaque	75	Smooth
White Granite	Heterogeneous: white with black crystals; opaque	28	Smooth
Black Coal	Homogeneous: black; opaque	50	Smooth
Concrete	Homogeneous: grey; opaque	60	Rough
Limestone Block	Homogeneous: cream; opaque	24	Rough
Basalt	Homogeneous: black; opaque	13	Smooth
Laterite	Heterogeneous: orange with brown and black crystals	24	Smooth with a few holes
White Quartz	Homogeneous: white with linear black mineral intrusions; translucent	24	Smooth

The irregularly shaped rock specimens were cut with a rock saw to give a smooth, planar surface to scan and hence minimise scattering due to diffuse reflection. The concrete and limestone block samples had planar faces resulting from their manufacture, but were somewhat rougher than the cut rock surfaces. The cut face of the laterite sample possessed a few holes due to its large (e.g., visible) crystal structure. The expected consequence of these textures was increased diffuse scattering.

Several types of retro-reflective surveying targets were also scanned, including a standard EDM prism, cat eye targets (both white and red) and traffic reflectors. Strong returns were expected due to their retro-reflective nature.

The geometry of the experiment is illustrated in Figure 1. Each rock sample was placed on a plane table at the same height as the scanner with its planar surface vertical and normal to the scanner's Z-axis to ensure normal incidence of the laser. The planar surface of each rock was carefully aligned with the table edge and levelled using a setsquare. Each rock was shimmed in place for scanning with a tack adhesive. These measures were taken with the view to positioning each sample at the same spatial distance from the scanner. The planar surface of each specimen was located 0.612m in front of a wall.

Independent measurements with a steel ruler were taken to ensure that each specimen was accurately oriented. Any observed range differences between samples could then be attributed to material effects on the reflected signal.

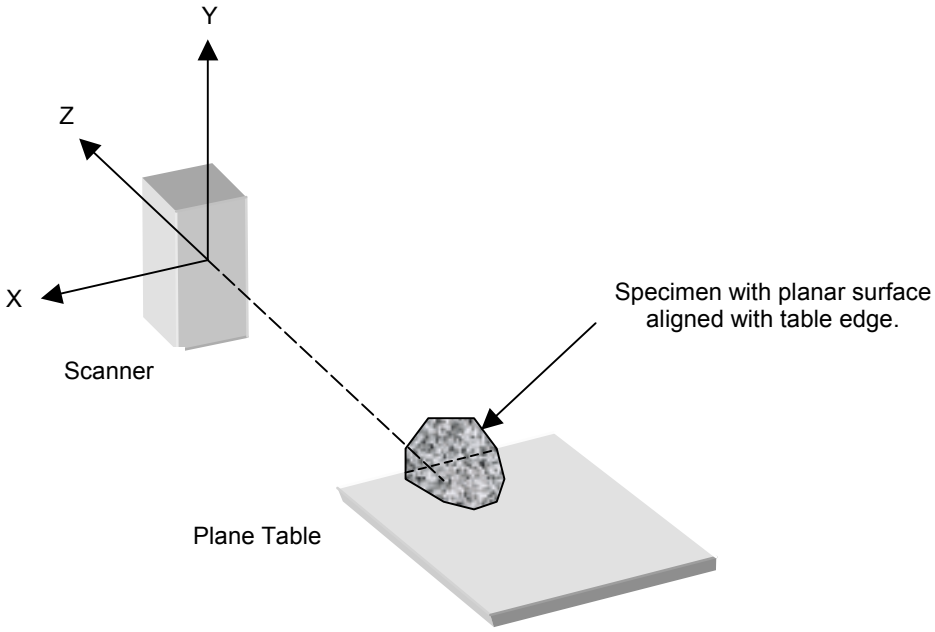

Figure 1. Experiment Setup.

Two scans of each sample were captured: one dry and one wet. A film of water was applied to the reflective planar surface with a squirt bottle without moving the specimen to ascertain the effects of surface moisture on range measurement. The time between water application and scan completion was on the order of a few minutes.

The experiment was conducted at two ranges: 3m (close range) and 53m (medium range). The latter was chosen since the ±6mm Cyrax positioning accuracy is quoted for ranges up to 50m. The close range experiment was conducted indoors, whilst the medium range testing was performed outdoors due to space limitations. Temperature was measured at the time of each scan, though the first velocity correction was insignificant in every case. Each surface was scanned with a nominal sampling interval of 2mm in both the x and y dimensions. This provided several hundred measurements per specimen. In some cases, more than one thousand samples were acquired. The resulting point clouds were edited so that only the returns from the planar reflecting surface were retained for data analysis.

The samples were chosen for their range of colour and mineral composition. Colour indicates the region of the visible spectrum the specimen reflects most strongly. Given the variety of colours one would expect each to exhibit different reflectance (Eq. 3). It is worth noting that none of the specimens were green, the colour of the Cyrax laser. Most samples had homogeneous mineral composition, with the exceptions being the white granite and the quartz. The former had a black and white speckled colour, though the crystals were much smaller (i.e., a few millimetres across) than the laser spot (≈5-6mm). The quartz was translucent white with a linear, black mineral intrusion. The translucence gave rise to the possibility of internal scattering of the laser (c.f. Godin *et al.*, 2001).

4. Results and Analysis

4.1 Range and Intensity at 3m

Analysis of the 3m experiment findings revealed that differences in mean range (-Z) were present between samples, but were at the level of individual point standard deviations, which ranged from ±4 to ±9mm. Though possibly due to material differences, they can most likely be attributed to alignment errors in specimen placement. Differences between the wet and dry measurements, which were not subject to alignment errors, were on the order of 1-2mm (with basalt being the exception at 6mm), much lower than the individual point standard deviations. No significant differences existed between the dry and wet standard deviations.

Three repeat scans of the red brick were obtained prior to the dry and wet surface testing. The brick was not moved between scans in this case. No differences existed in the first two moments of the range (-Z) and intensity (E) data. Figure 2 shows the histogram of range and intensity measurements for the red brick repeatability test. In each case, the range histogram has a negatively skewed shape, indicating that shorter ranges were more probable than longer ranges. Each histogram also exhibits a bimodal structure. A local maximum is visible at approximately Z=-3.07m, particularly in scans 1 and 3. The bimodal appearance suggests that multiple returns were received from the red brick. The physical reason for this behaviour is not known, as the brick surface was planar and returns from surrounding objects were removed prior to analysis. The intensity histograms each have a unimodal, positively skewed shape.

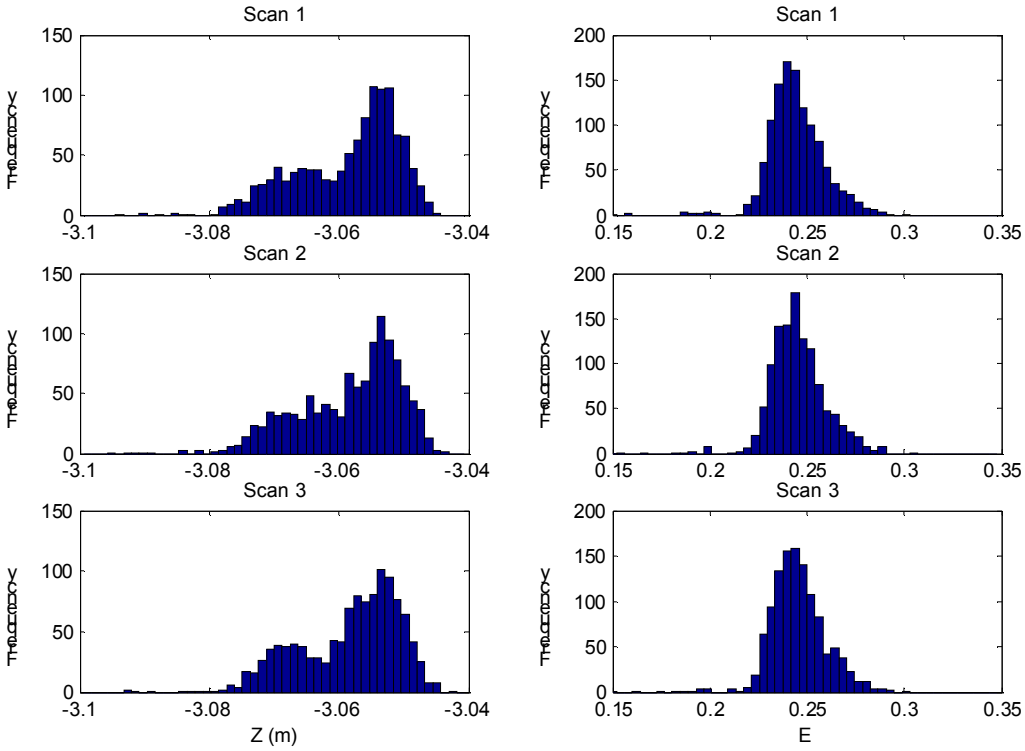

Figure 2. Range (-Z) and Intensity (E) Histograms from the Red Brick Repeatability Tests.

Plotted in Figure 3 are the dry and wet surface range histograms of three different materials. Though slightly different in appearance, all exhibit a negatively skewed shape. The red brick histogram is similar to those in Figure 2, though the secondary peak is less pronounced. The effect of surface moisture appears to be a slight transformation of histogram shape, which is most evident for the black coal specimen. However, it must be recalled that there was no significant change to the first two statistical moments of the range for these samples.

Since mean intensity was the most significantly affected statistic, wet and dry results at both ranges are presented in Table 2. Full reporting of the results can be found in Lichti and Harvey (2002). Not surprisingly, the white and cream coloured materials exhibited the greatest dry surface reflectance at 3m as indicated by the intensity attribute. For example, the mean intensity of the white limestone was 0.39. Also not surprising was the low reflectance of the black coal, for which mean intensity was 0.17. The addition of surface moisture had more of an effect on some samples than on others, with no colour or surface finish dependence visible. However, due to variations in surface finish among the specimens, reflectance differences were attributed to a combination of material properties and surface roughness. Intensity standard deviation increased as a result of applying water to the reflecting surface (e.g., white granite: ±0.05 dry, ±0.16 wet), with the exception of two cases (limestone block and red brick) where no change was observed. Interestingly, a dramatic increase in basalt mean-intensity was observed (0.30 dry, 0.59 wet). Many samples with an intensity of 1.0 were recorded, which indicated detector saturation.

Figure 4 shows the intensity histograms of the dry and wet surfaces for the same specimens from Figure 3. In each case, the dry histograms have a positively skewed shape. The dry red brick histogram-shape closely resembles those of Figure 2. The wet surface histograms show much greater dispersion. Several local maxima at higher intensity values are also visible.

Table 2. Mean Intensity Summary.

Specimen	Mean Intensity			
	3m		53m	
	Dry	Wet	Dry	Wet
Red Brick	0.25	0.22	0.14	0.12
Limestone	0.39	0.46	0.28	0.25
White Granite	0.35	0.42	0.22	0.18
Black Coal	0.17	0.25	0.10	0.13
Concrete	0.30	0.25	0.16	0.15
Limestone Block	0.37	0.36	0.27	0.23
Basalt	0.30	0.59	0.14	0.13
Laterite	0.26	0.29	0.14	0.13
White Quartz	0.32	0.35	0.18	0.18

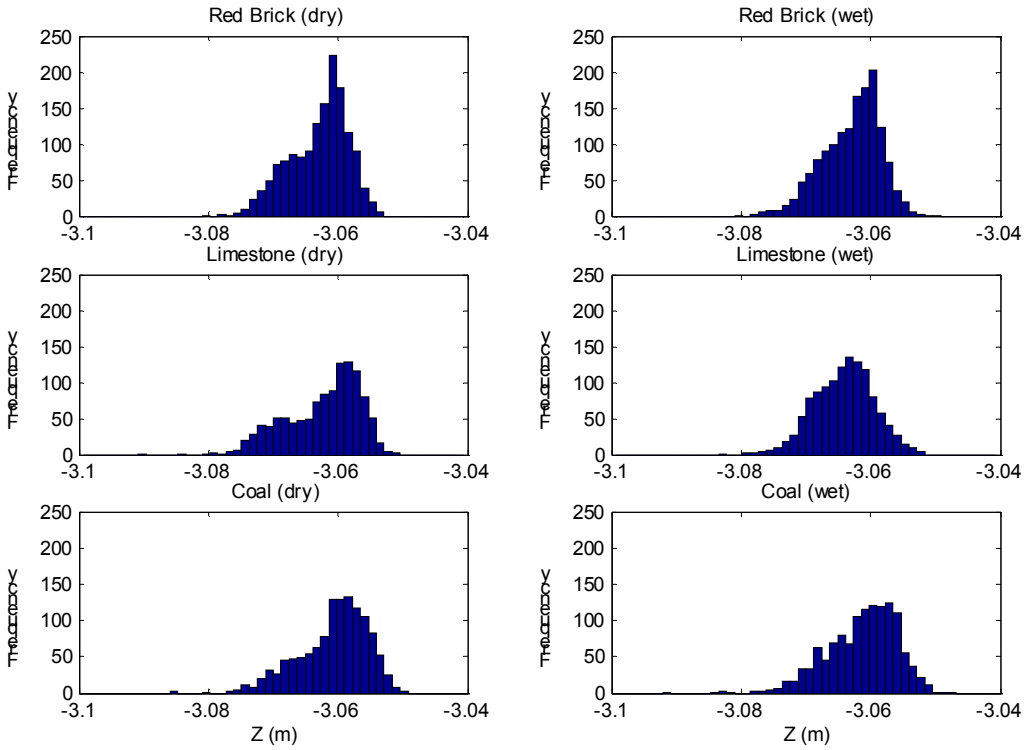

Figure 3. Range (-Z) Histograms for Three Materials at 3m, Dry and Wet.

4.2 Range and Intensity at 53m

The magnitudes of range (-Z) point standard deviations at 53m were commensurate with those at 3m. Some differences existed in range on the order of point standard deviation magnitude. These results were subject to alignment errors and less well-controlled atmospheric conditions (outdoors) over the 106m optical paths. Differences in mean range of up to 3mm were observed between wet and dry samples.

As with the 3m test, the white and cream coloured materials exhibited the greatest dry reflectance at 53m (e.g., limestone mean intensity was 0.28). Once again, the black coal exhibited the lowest mean intensity at 0.10. Intensity values at 53m were generally lower, likely due to greater atmospheric attenuation over the longer path and, in general, were about half the intensity of the same material at 3m. In contrast to the close range experiments, application of surface moisture caused a

decrease in mean intensity, with few exceptions. No increase in intensity standard deviation was observed due to surface moisture, as was the case at 3m.

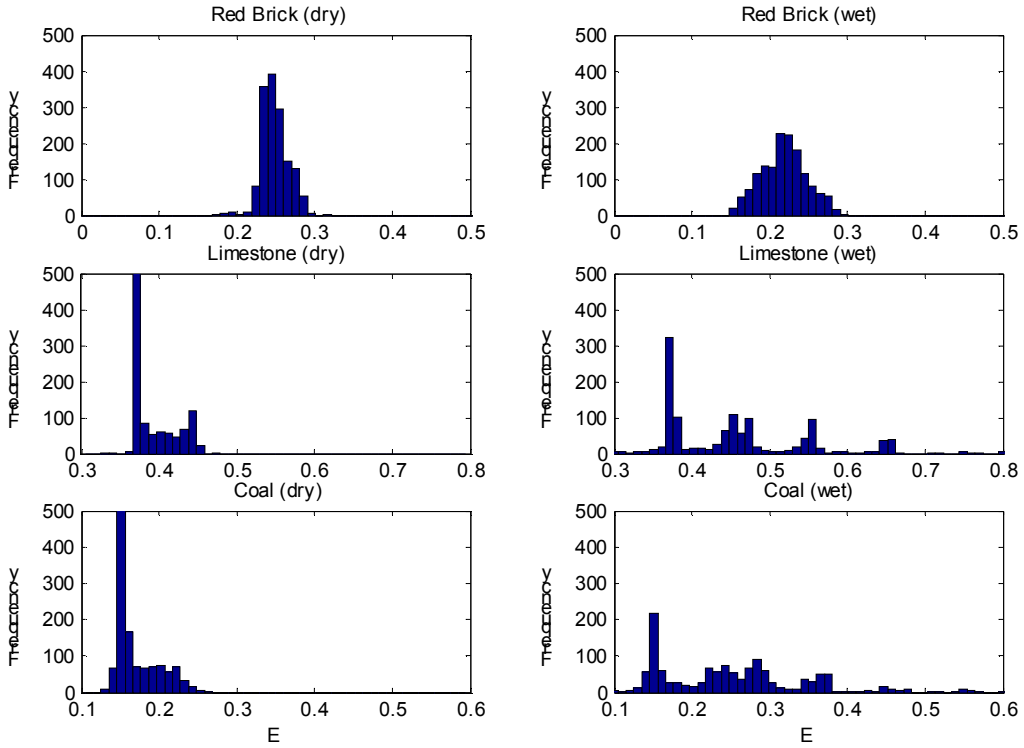

Figure 4. Intensity (E) Histograms for Three Materials at 3m, Dry and Wet.

4.3 Scanning of Survey Targets

No results have been presented for the scans of the surveying reflectors. Due to their retro-reflective nature, most laser returns saturated the Cyrax's photodetector, which yielded intensity attribute values of 1.0. Visual inspection of the point clouds revealed significant range biases due to the saturation at both 3m and 53m. This would suggest that traditional survey targets are not appropriate for use with laser scanners.

4.4 Imaging the Laser Spot

Pictured in Figure 5 is an image of the Cyrax 2400 laser spot projected onto a proprietary Cyra target. The target consists of an 8 x 8cm square of green film and a 3cm diameter white circle. The image was captured with a digital camera during a high-density scan of a small region of the target. The spot is slightly elongated in the vertical dimension due to its upward scanning motion during image exposure. Since the camera was operated in automated mode, the exposure settings were not available. Clearly, though, the shutter speed was slower than the 1000Hz scan-rate. The spot visible in Figure 5 is likely the superposition of several spots.

The spot diameter in the direction orthogonal to the scan motion was measured to be approximately 5.5mm, which agrees with the Cyra specification that it is less than 6mm for the range 0-50m. It is important to note that the distribution of irradiance within the laser beam spot is not uniform but Gaussian, so no distinct point of reference exists for a diameter definition. Several spot diameter definitions exist, with the most common being the $1/e^2$ irradiance level diameter (Matthews and Garcia, 1995).

The spatial fluctuations of spot intensity are due to speckle noise, a random interference pattern inherent to laser imaging systems caused by surface roughness on the scale of the laser wavelength. The horizontal intensity cross-section extracted from the digital image brightness values, plotted in Figure 6 (the image pixel spacing was 9μm), also shows the speckle noise. Note that the intensity profile is clipped at 255 due to saturation of the camera's CCD detectors. If not clipped, the

profile trend would exhibit a Gaussian shape. The profile floor (BV≅50) represents the reflection of ambient light by the green target film.

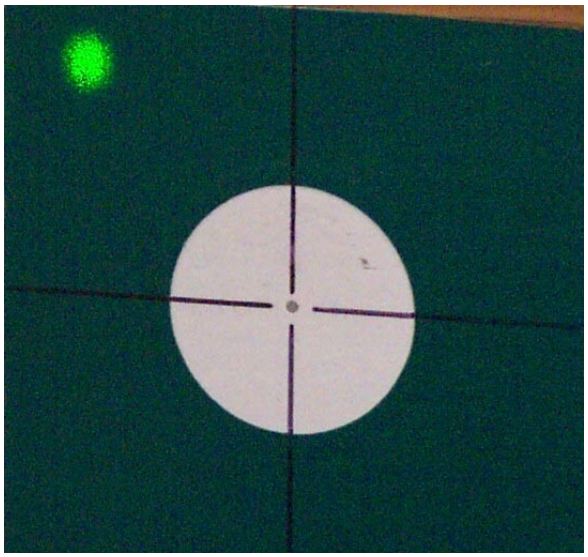

Figure 5. Image of Cyrax Laser Spot on a Cyra Target.

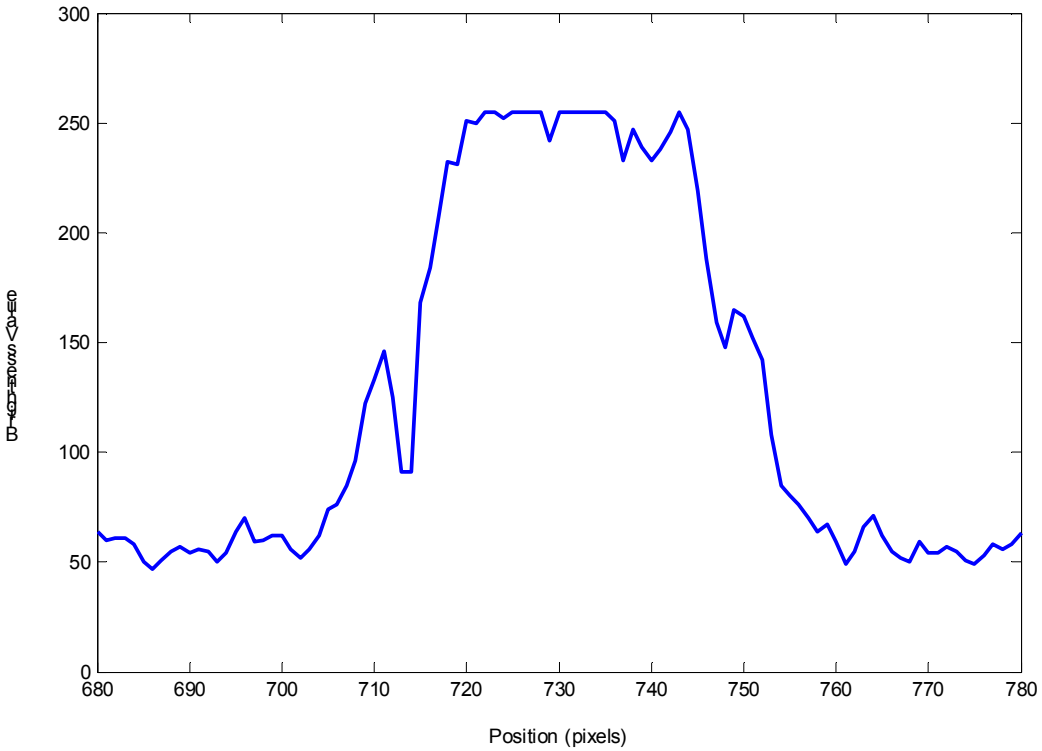

Figure 6. Laser Spot Horizontal Cross-Section.

5. Conclusions

A set of experiments has been conducted in an attempt to quantify possible range errors from a TOF scanner system due to reflecting surface material properties. Measurements were successfully obtained from all materials at all ranges; no

problems with lack of returns were encountered as in Gordon *et al.* (2001). Though differences between specimens were observed, they could not be attributed to material properties due to possible alignment errors. Range differences between wet and dry specimen measurements that were immune to alignment errors were observed. However, since they were at or below the precision of individual range measurements, they were deemed insignificant. The lack of range errors may be due to return pulse amplitude adjustment performed by the scanner electronics.

Intensity attribute differences were observed between specimens and between dry and wet surfaces. At close range, intensity increased in most cases when the reflecting surface was wet. At medium range, most samples exhibited a decrease in intensity when wet. The practical consequence of this outcome is possible reduction in maximum scanning range if the reflecting surface is wet. An increase in intensity attribute dispersion measured was observed for wet surfaces at 3m, but not at 53m. The increase at 3m may be due to the water film being the dominant reflector. That the effect was not observed at 53m may be due to a greater evaporation rate outdoors. As well as dry and wet effects, intensity decreases with an increase in distance to the target. In general, intensity at 53m was found to be about half the intensity of the same material at 3m.

Histogram analysis indicated that the ranges over small, planar surfaces normal to the scanner axis followed a non-symmetric distribution, for which near ranges were more probable than far ranges. The analytical form of the probability density function of the range observations is a function of errors in the wave front (e.g., speckle) and the method of detection used by the Cyrax system, i.e., incoherent or coherent detection (Andrews *et al.*, 2001). The effects of surface moisture were found to be a slight shape alteration to the histogram of ranges and significant alterations to the intensity histogram.

In another part of the experiments, the Cyrax laser spot was imaged with a digital camera. The capture of this image gives rise to the possibility of three-dimensional spot positioning, say via digital photogrammetry or theodolite direction measurements. This would be useful for independent accuracy assessment and development of calibration procedures and is the focus of ongoing research.

References

Amann, M-C, T Bosch, M Lescure, R Myllylä and M Rioux (2001) Laser ranging: a critical review of usual techniques for distance measurement. *Optical Engineering.* 40(1): 10-19.

Andrews, L C, R L Phillips and C Y Hopen (2001). *Laser Beam Scintillation with Applications.* SPIE Press: Bellingham, WA.

Balzani, M, M Pellegrinelli, N Perfetti, P Russo and F Uccelli (2001) Terrestrial 3D laser scanner: preliminary accuracy tests. In *Proceedings of the Italy-Canada 2001 Workshop on 3D Digital Imaging and Modeling Applications in Heritage, Industry, Medicine and Land.* 8 pp.

Fowles, G R (1975) *Introduction to Modern Optics.* Second edition. Dover Publications Inc: New York, NY.

Godin, G, M. Rioux, J-A Beraldin, M Levoy, L Cournoyer and F Blais (2001) An assessment of laser range measurement of marble surfaces. In *Optical 3-D Measurement Techniques V.* 1-4 October 2001, 49-56.

Gordon, S J, D D Lichti, M P Stewart and M Tsakiri (2001) Metric performance of a high-resolution laser scanner. In *Videometrics and Optical Methods for 3D Shape Measurement,* 22-23 January 2001, 174-184.

Jelalian, A V (1992) *Laser Radar Systems.* Artech House: Boston, MA.

Kurisake, N, W Che and T Nakane (2001) Applications of 3D measurement with ground laser scanner. In *Videometrics and Optical Methods for 3D Shape Measurement,* 22-23 January 2001, 101-106.

Lichti, D D and B R Harvey (2002) An investigation into the effects of reflecting surface material properties on terrestrial laser scanner measurements. *Geomatics Research Australasia* (In press).

Lichti, D D, M P Stewart, M Tsakiri and A J Snow (2000) Benchmark testing on a three-dimensional laser scanning system. *Geomatics Research Australasia* 72: 1-23.

Matthews, L and G Garcia (1995) *Laser and Eye Safety in the Laboratory.* IEEE Press: Piscataway, NJ.

Runne, H, W Niemeier and F Kern (2001) Application of laser scanners to determine the geometry of buildings.. In *Optical 3-D Measurement Techniques V.* 1-4 October 2001, 41-48.

Ullrich, A, R Reichart, R Schwarz and J Reigl (2001) Time-of-flight based 3D imaging sensor with true-color channel for automated texturing. In *Optical 3-D Measurement Techniques V.* 1-4 October 2001, 2-9.

Wolfe, W L (1998) *Introduction to Radiometry.* SPIE Optical Engineering Press: Bellingham, WA.